ENSO and the seasonal cycle of precipitation in Southeast Asia

Alessandra Giannini, IRI

Abstract

We apply Principal Component Analysis to the study of the seasonal cycle of precipitation over Southeast Asia (20°S to 20°, 90°E to 180°E) to aid in a concise and quantitatively informative characterization of features relevant to agricultural practice, such as onset of the rains, timing of floods, and onset of the dry season. As an example, we discuss the impact of ENSO warm and cold phases on these features for two locations in Indonesia; the rice-growing district of Indramayu in Jawa Barat, and the semi-arid province of Nusa Tenggara Timur.

IRI, February 2005

1 Introduction

The El Niño-Southern Oscillation (ENSO) is unquestionably the dominant pattern of interannual climate variability in the Southeast Asian/Western Pacific region. When, in a warm ENSO event, the location of deep convection shifts from the maritime continent to the central and eastern equatorial Pacific, vast portions of Indonesia, the Philippines, Papua-New Guinea and eastern Australia, as well as many Pacific Island states, experience drought. However, when compounded over the lifecycle of an ENSO event, from July of the year of onset, or year (0), to June of the following year, or year (1), persistent, statistically significant rainfall anomalies are seen to be limited geographically to the more equatorial regions of Indonesia and the Philippines, sparing, for example, the highly densely populated island of Java (Figure 1). Furthermore, it is features in the seasonal cycle of precipitation such as onset of the wet and dry seasons and the intra-seasonal distribution of rainfall, rather than the total seasonal or annual amount, that are of greatest concern to users of climate information in the agricultural production sector. A false start to the wet season can precipitate seeding, and lead to loss of seeds, and to increased labor due to the necessity to repeat seeding or transplanting of seedlings. An early start to the dry season can impact the crop in the ground, preventing full maturation.

Recent advances in dynamical seasonal climate prediction (Goddard et al 2001; Barnston et al 2003) have made possible the probabilistic forecast of total seasonal amounts of rainfall with a lead time of a month to a year. But knowledge of the relationship between the large-scale patterns of variability that inform the predictability of climate, and the intra-seasonal distribution of the rains -

knowledge so crucial to agricultural practice - is still wanting, primarily due to the lack of substantive, quantitative studies.

Understanding how features of the seasonal cycle of precipitation such as onset date of the wet and dry seasons vary from year to year in accord with large-scale climate phenomena such as ENSO is key to their prediction. In the context of a project on *Climate forecast applications for disaster mitigation in Indonesia, Philippines, and Vietnam*, the International Research Institute for climate prediction (IRI; *http://iri.columbia.edu*), together with its partners in region[1], is undertaking research to substantiate the evidence base for the exploitation of climate information in agriculture, and to facilitate its uptake in the design of livelihood strategies in the face of climate risk.

The purpose of this technical note is to present an application of Principal Component Analysis (PCA) to the study of features of the seasonal cycle in Southeast Asia of relevance to agricultural practice. In the next section, we briefly present data and methods. In section 3, PCA is applied to the seasonal cycle of global, tropical surface temperature and precipitation, and of precipitation only over Southeast Asia. In section 4, the impact of ENSO on the seasonal cycle is described in terms of the leading modes of the seasonal PCA of precipitation. Section 5 summarizes and concludes.

[1]The project is coordinated by the Asian Disaster Preparedness Centre (ADPC; *http://www.adpc.net*), headquartered in Bangkok, Thailand. Partners in Indonesia include Badan Meteorologi dan Geofi sika (BMG, the Bureau of Meteorology and Geophysics; *http://www.bmg.go.id*), and Institut Pertanian Bogor (IPB, Bogor Agricultural University; *http://www.ipb.ac.id/*).

2 Data and Methods

This note is concerned with the application of Principal Component Analysis (PCA; Preisendorfer 1988; Peixoto and Oort 1992; von Storch and Zwiers 1999) to global datasets of surface temperature and precipitation. These datasets are made publicly available through the IRI Data Library webserver (*http://iridl.ldeo.columbia.edu/index.html*). Surface temperature is extracted from the NCEP/NCAR Reanalysis (Kalnay et al 1996) and precipitation is extracted from NASA's Global Precipitation Climatology Project (GPCP; Huffman et al 1997) and from NOAA's Climate Prediction Center (CPC) Merged Analysis Product (CMAP; Xie and Arkin 1997).

PCA is a statistical technique routinely used in the analysis of geophysical data that is particularly valuable in separating signal from noise, and, when successful, in isolating the signal in a few, highly spatially coherent patterns.

The first step to applying PCA to the analysis of the seasonal cycle (Stidd 1967; Giannini et al 2000) is to form a data matrix of the climatological mean seasonal cycle at each station or grid point. The number of rows in this data matrix is equal to the number of stations or grid points in the geographical domain of interest, while the number of columns is equal to the number of monthly, dekad, pentad or daily time steps in a year, depending on the temporal resolution of the dataset to be analyzed. Seasonal anomalies are formed by removing the annual mean at each location, i.e. from each row. Annual mean surface temperature and precipitation for the Southeast Asian region are depicted in Figure 2. If the annual mean is not removed, then the leading pattern extracted by PCA will capture it. In the PCA

decomposition of the covariance matrix of such a data matrix the spatial patterns are often referred to as Empirical Orthogonal Functions, or EOFs, the time series as Principal Components, or PCs.

In the global tropical calculations of Section 3, PCA is applied to the seasonal cycle computed from monthly climatologies obtained by averaging over 1979-2003, the period common to NCEP/NCAR, GPCP and CMAP. In the calculations pertinent to the seasonal cycle of precipitation over Southeast Asia, in Sections 3.1 and 4, the higher temporal resolution pentad (5-day) product of CMAP is used.

3 Applying PCA to the study of the seasonal cycle in the tropics

When PCA is applied to the seasonal cycle of temperature (Fig.3) or precipitation (Fig.4) in the tropics (20°S to 20°N), it typically identifies components with annual periodicity in the first couple of modes. Since these modes are orthonormal by construction, their associated time series will appear *in quadrature* to each other, or approximately offset by 90°. Typically, the first PC represents the extremes in seasonality, with maximum and minimum close to the solstices, while the second PC represents the transitional seasons, with maximum and minimum close to the equinoxes. Components that have a semi-annual period, related to the sun's two overhead passings in one year, are important locally, especially near the equator, but typically explain smaller fractions of variance, hence they are relegated to higher-order eigenvectors.

The first three components of the seasonal cycle respectively capture 97% and 89% of the variance

in tropical surface temperature (Fig.3) and precipitation (Fig.4). In such a situation, i.e. when PCA compounds a large fraction of the variance in the first few patterns, one can rightfully limit consideration to those first few patterns to characterize variability. In other words, this situation is equivalent to truncating the reconstruction of the variable (X, in the equation below) in terms of EOFs and PCs to the first few orthonormal components:

$X(x,t) = \sum_{i=1}^{N} EOF_i(x) \cdot PC_i(t) \simeq \sum_{j=1}^{K} EOF_j(x) \cdot PC_j(t)$, where $K \ll N$

(In the above, x is the spatial dimension, t is the temporal dimension.)

The leading pattern of the PCA of surface temperature, which alone accounts for 65% of the variance, is a 'solstice' pattern, representing the maximum heating/cooling of the continents attained in local summer/winter. The second pattern, which accounts for 27% of the variance, is an 'equinox' pattern, representing the contrast in land/ocean temperature due to the difference in thermal inertia between the two media. When the ocean is at its warmest, approximately 3 months after the summer solstice, or in local autumn, the continents have already considerably cooled. Conversely, the ocean attains its coolest surface temperature in local spring, when the land is already warming up as the solstice maximum approaches. The third component is a semi-annual pattern, accounting for 5% of the variance.

The leading pattern of the PCA of precipitation, which alone accounts for 67% of the variance, is a 'monsoon' pattern. It is antisymmetric about the equator, and has extrema in July and February, i.e. approximately one month after the solstices. The second pattern, which accounts for 15% of the

variance, is a 'transition' pattern. It is symmetric about the equator in the central and eastern Pacific and western Atlantic basins, with maximum in April-May, and in the Indian and western Pacific basins, with maximum during the 'northeastern monsoon', in October-December. It is antisymmetric about the equator across Africa, where it can be characterized as a prelude to the poleward expansion, and equatorward retreat of the monsoon in spring and fall respectively. The third component captures 7% of the variance, and is semi-annual in period.

3.1 PCA of precipitation over Southeast Asia

In Figure 5 we show results from PCA applied to CMAP pentad precipitation over a tropical Southeast Asian domain (20°S to 20°N, 90°E to 180°E). When care is taken to define a geographical domain that spans the equator on both sides, the first spatial pattern in the PCA of the seasonal cycle of precipitation (with the annual mean removed) is a *monsoon* pattern. In the case of Southeast Asia it explains 54% of the total variance. As in its global tropical counterpart, spatial loadings have opposite sign on opposite sides of the equator (Fig.5a). The extrema in the associated time series (Fig.5b) occur approximately one month after the June and December solstices.

The second spatial pattern (Fig.5c) explains 9% of the total variance. It is, again, a *transitional* pattern. In the southern hemisphere, from southern Sumatra and Java to the island of Timor and northern Australia, it represents an early start to the rainy season, in local spring. In the northern hemisphere it captures the late end of the rainy season, related to the northeasterly monsoon. The

latter feature is most notable in maxima along the northeast-facing coasts of the Philippines, Vietnam and Malaysia.

The third spatial pattern (Fig.5e) explains 7% of the total variance. It is a *semi-annual* pattern, adding amplitude to the maximum in the monsoonal pattern in regions farther away from the equator, and to the maximum in the transitional pattern in regions closer to the equator.

4 ENSO-related variations in the seasonal cycle

As seen in the previous section, the power of PCA lies in its ability to efficiently synthesize information. PCA paints a broad-brush picture with a few strokes, allowing identification of homogeneous regions at a glance. In this section we showcase the power of PCA by applying it to the study of variations in the seasonal cycle associated with ENSO phases, the dominant driving force of climate variability across Indonesia.

ENSO years are here defined based on the December(0)-January(1) value of Niño-3 - the anomalous sea surface temperature in the central and eastern equatorial Pacific (5°S to 5°N, 150°W to 90°W). When such value is greater than 1°C, or less than -0.75°C, the year from July(0) to June(1) is classified as a warm or cold ENSO year. The remaining years are classified as neutral. Over the time period covered by CMAP (1979 to 2003) 1982-83, 1986-87, 1987-88, 1991-92, 1994-95, 1997-98 and 2002-2003 are identified as warm ENSO years, and 1984-85, 1988-89, 1998-99 and 1999-2000 are

identified as cold ENSO years.

Because the first three leading patterns capture a considerable portion of the total variance of Southeast Asian rainfall, i.e. on the order of 70%, we assume that a truncated reconstruction of the seasonal cycle of precipitation, i.e. one limited to the first three leading patterns only, is a plausible approximation. Hence we limit our consideration to them. We start by projecting the three leading spatial patterns of the seasonality of precipitation over Southeast Asia (Figures 5a,c and e) separately onto the averages of warm, cold and neutral ENSO years. The *monsoon*, *transitional* and *semi-annual* components of the seasonal cycle in warm ENSO, cold ENSO and neutral years can be compared in Figure 6. Noteworthy features are:

- in the monsoon component (Fig.6a) the (southern hemisphere) dry season is drier than average during year(0) of a warm ENSO, especially during July-August. During a cold ENSO it is comparably not as dry.

- still in the monsoon component, following the mature phase of a warm ENSO event the onset of the dry season is delayed. It comes earlier following a cold ENSO event.

- in contrast to the monsoon component, the *transitional* component (Fig.6b) shows increased rainfall during the transition season (August-September) of a warm ENSO event.

- in the core region of the southern hemisphere monsoon, centered at 10°S between Indonesia, Papua/New Guinea and northern Australia, the semi-annual component (Fig.6c) partially coun-

teracts the monsoon pattern during the dry season. Conversely, it significantly contributes to the anomalous dry signal during the transition and wet seasons of a warm ENSO, in October-February.

4.1 Reconstruction of the seasonal cycle at locations in Indonesia

To quantify the regional-scale impact of ENSO on the seasonal cycle, it is useful to reconstruct a 'truncated' seasonal cycle at one location based on knowledge of the annual mean and of spatial loadings associated with only these three leading patterns. Two examples are illustrated in Figure 7, namely Indramayu and Nusa Tenggara Timur.

According to the GPCP/CMAP climatologies, annual-mean monthly rainfall in western Java, where the district of Indramayu is located, is 150 mm/month. The spatial loadings of PCs 1, 2 and 3 (see Fig.5) are 1, 0.5 and 0.5, respectively. Hence, a simple reconstruction of the typical seasonal cycle in Indramayu is given by:

$$Indramayu = 150 + 1.0 * PC1 + 0.5 * PC2 - 0.5 * PC3$$

Nusa Tenggara Timur is farther away from the equator, at around 9°S. Conditions are overall drier, as exemplified by a smaller annual mean value of 120 mm/month, and the amplitude of the seasonal cycle is more pronounced, as exemplified by the larger spatial loadings of PCs 1, 2 and 3, which are closer to 1.5, 0.5 and 1.2 respectively. Hence the typical seasonal cycle in Nusa Tenggara Timur can be reconstructed as:

$$NusaTenggaraTimur = 120 + 1.5 * PC1 + 0.5 * PC2 + 1.2 * PC3$$

Based on this analysis, we can conclude that in Indramayu the strongest signal associated with a warm ENSO event is in the drier than average dry season during year(0) of a warm ENSO, i.e. in the July-August prior to the mature ENSO phase in October-December. Conversely for a cold ENSO event. Secondly, there is a tendency towards a delayed onset of the dry season in the March-April following a warm ENSO event. Conversely, following a cold ENSO event, the onset of the dry season is hastened. However, no apparent difference is noted in rainfall amounts at the peak of the rainy season.

In Nusa Tenggara Timur, we note the flip-flopping in sign of the signal during the dry and transition seasons (July-October). This behavior is consistent with local knowledge of a 'false start' to the rainy season as a potential climate problem (Someshwar, personal communication). In the case of a warm ENSO event, following such a false start rainfall is reduced during the early months of the rainy season (November-December).

5 Summary and conclusions

We presented an application of Principal Component Analysis, a tool widely used in the analysis of large geophysical datasets, to aid in the statistical characterization of the dependence of the seasonal cycle of precipitation on large-scale patterns of climate variability. The specific problem we addressed

was the impact of ENSO on the seasonal cycle of precipitation over Indonesia, but this tool can be easily generalized to the study of the impact of any large-scale pattern of climate variability on any other region of the world.

The motivation stemmed from the observation (Fig.1) that despite ENSO's well-known impact on the climate of the maritime continent, when integrated over the canonical 1-year duration of an event, such impact is found to lose coherence away from the most equatorial latitudes. We find that for the rice-growing district of Indramayu, in Jawa Barat, this behavior is consistent with the observation that the impact of ENSO in terms of total rainfall at the beginning of the event, which coincides with the dry and transition seasons in Indonesia, is partially cancelled by that at the end of the wet season and beginning of the dry season. Presently the area planted in rice on the island of Java is reduced during the rainfall deficient dry and transition seasons leading to the mature phase of a warm ENSO event, and the loss is not made up for later on in the agricultural year (Naylor et al 2001). The oscillatory character of ENSO's impact here highlighted suggests that there may be potential for the improvement of agricultural yield during ENSO years.

The analysis for Nusa Tenggara Timur, a semi-arid province in southeastern Indonesia, lends credence to the local popular knowledge of a false start to the rainy season as a serious climate-related problem (Someshwar, personal communication). False starts typically occur in October/November, leading farmers to broadcast maize and rice. Crops can be damaged by subsequent prolonged dry spells.

Through this preliminary application, conducted on precipitation data of rather coarse spatial resolution, we hope to have demonstrated the potential usefulness of this statistical tool. We suggest that this tool undergo rigorous scrutiny, and that it be tested on locally available, high spatial resolution data before successful uptake into the decision-making system is warranted.

Acknowledgments ...

References

Giannini, A., Kushnir, Y. and Cane, M. A. 2000: Interannual variability of Caribbean rainfall, ENSO and the Atlantic Ocean. *J. Climate*, **13**, 297–311.

Goddard, L., Mason, S. J., Zebiak, S. E., Ropelewski, C. F., Basher, R. and A., C. M. 2001: Current approaches to seasonal to interannual climate predictions. *Int. J. Climatol.*, **21**, 1111–1152.

Huffman, G. J., Adler, R. F., Arkin, P., Chang, A., Ferraro, R., Gruber, A., Janowiak, J., McNab, A., Rudolf, B. and Schneider, U. 1997: The global precipitation climatology project (GPCP) combined precipitation dataset. *Bull. Amer. Meteor. Soc.*, **78**, 5–20.

Kalnay, E. and Coauthors 1996: The NCEP-NCAR 40-year reanalysis project. *Bull. Amer. Meteor. Soc.*, **77**, 437–471.

Naylor, R. L., Falcon, W. P., Rochberg, D. and Wada, N. 2001: Using El Ni˜no-Southern Oscillation climate data to predict rice production in Indonesia. *Climatic Change*, **50**, 255–265.

Stidd, C. K. 1967: The use of eigenvectors for climatic estimates. *J. App. Meteor.*, **6**, 255–264.

Xie, P. and Arkin, P. A. 1997: Global Precipitation: A 17-Year Monthly analysis based on gauge observations, satellite estimates and numerical model outputs. *Bull. Amer. Meteor. Soc.*, **78**, 2539–2558.

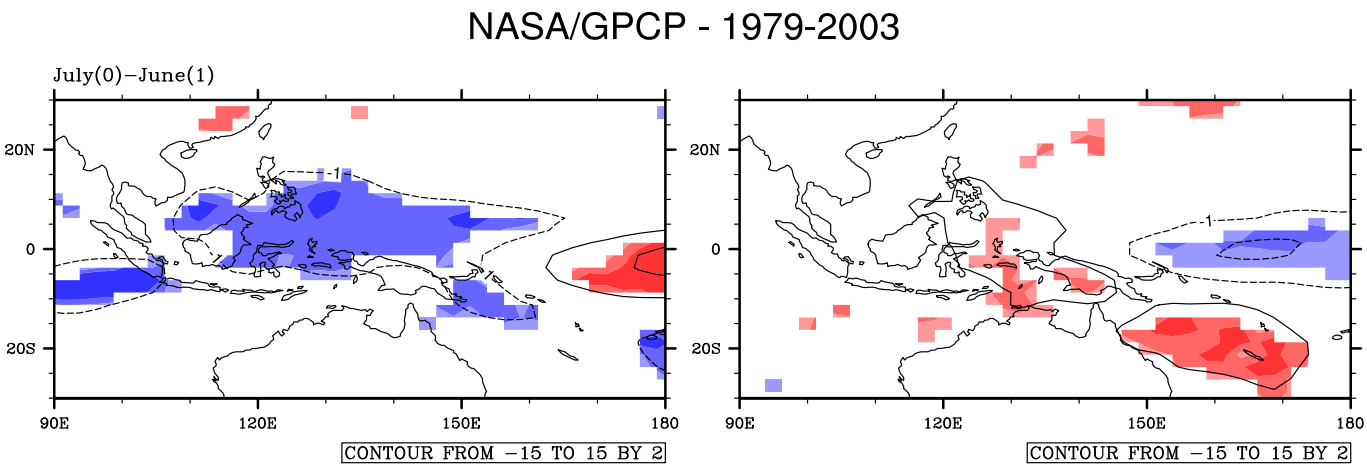

Figure 1: Warm ENSO minus neutral (left) and cold ENSO minus neutral (right) precipitation anomalies, July(0)-June(1) averages. Contour is every 2 mm/day, starting at 1 mm/day. Shading represents statistical significance at the 95% level or higher.

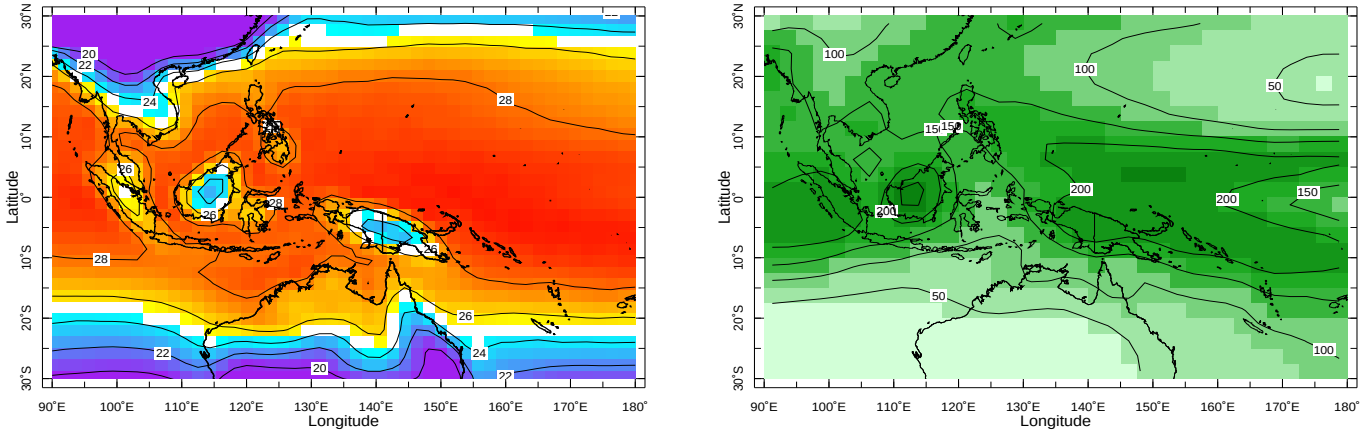

Figure 2: Annual mean surface temperature (left) and precipitation (right) in Southeast Asia

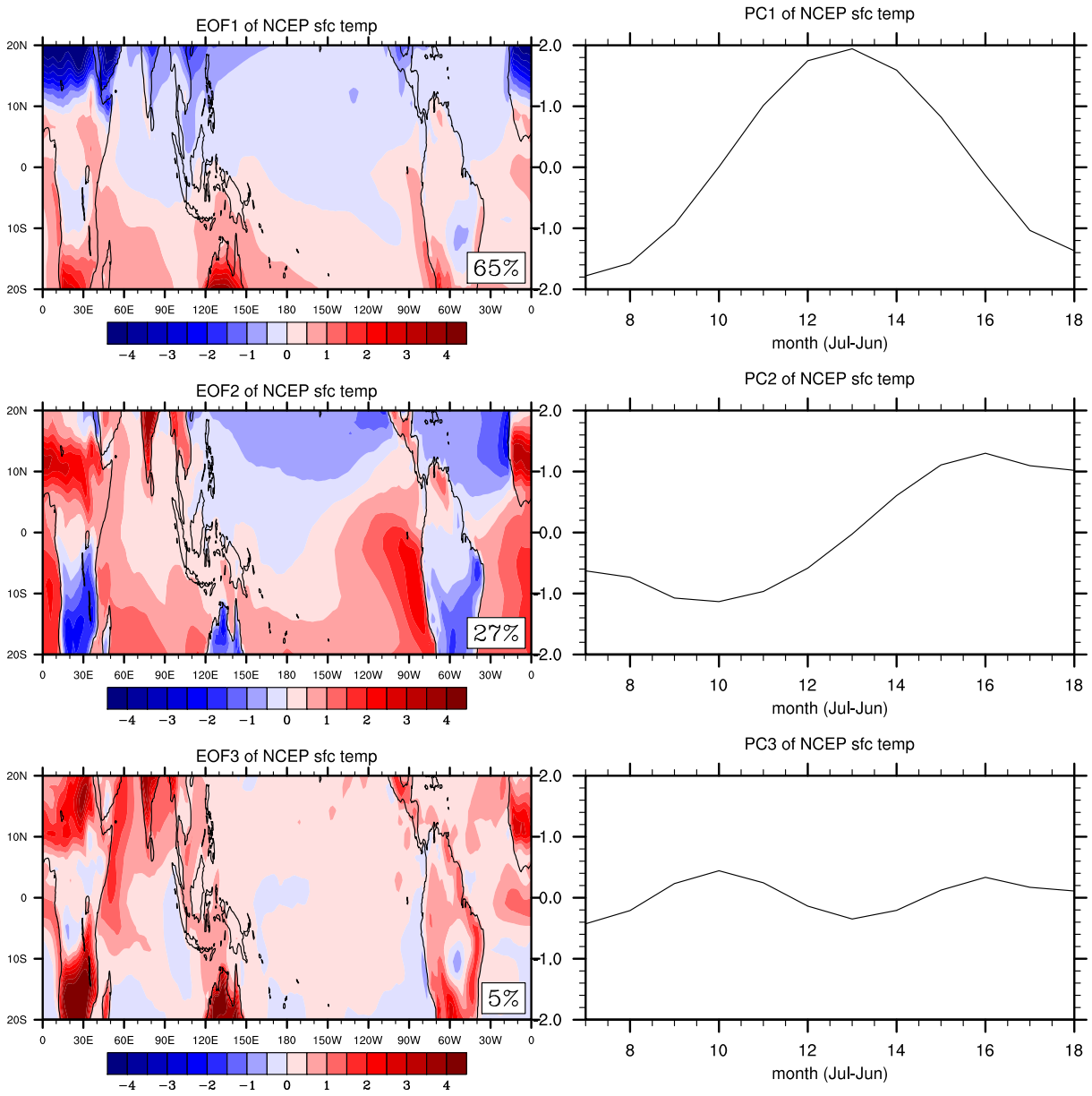

Figure 3: The first 3 EOFs/PCs of global tropical temperature, computed on NCEP/NCAR monthly surface temperature

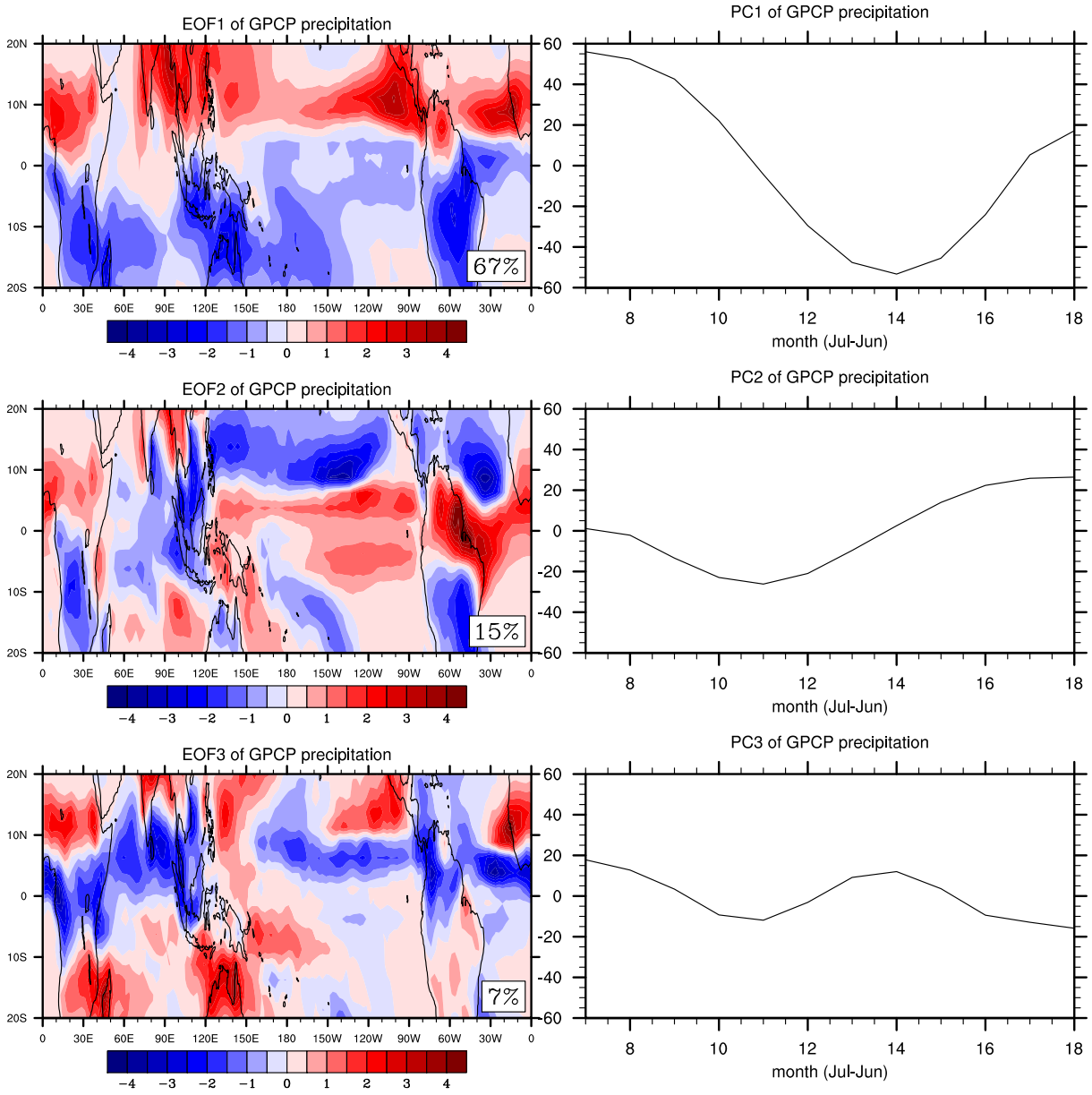

Figure 4: The first 3 EOFs/PCs of global tropical precipitation, computed on GPCP monthly precipitation

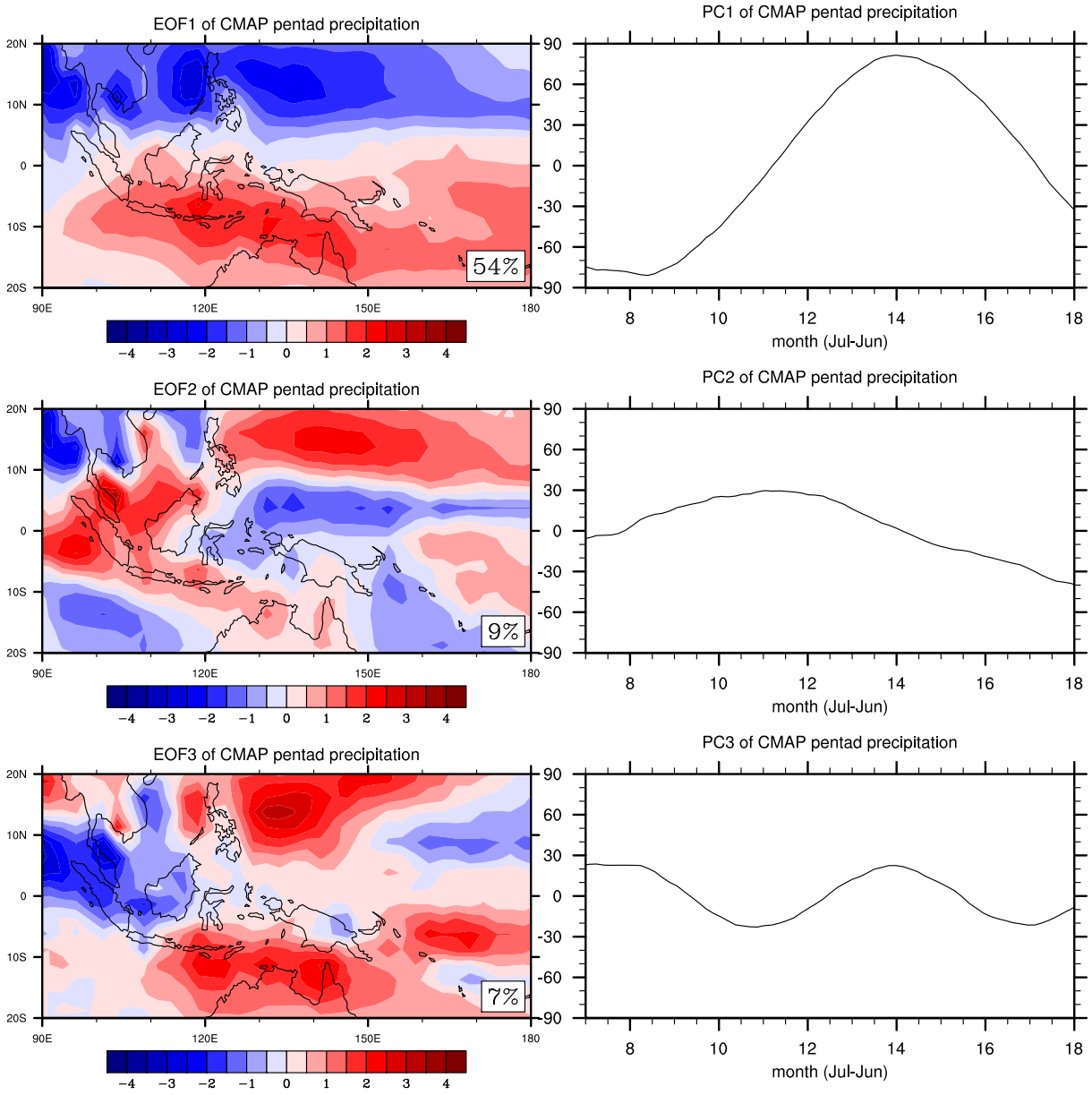

Figure 5: The first 3 EOFs/PCs of Southeast Asian precipitation, computed on CMAP pentad precipitation

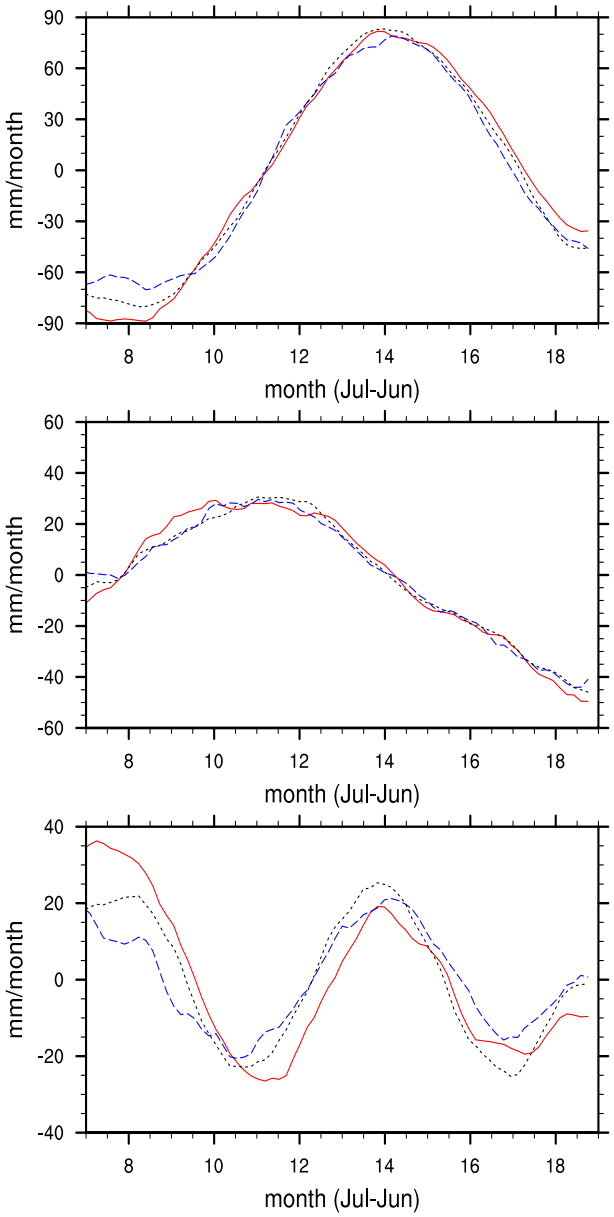

Figure 6: The three leading Principal Components of the Southeast Asian seasonal cycle of precipitation in warm ENSO (red/solid), cold ENSO (blue/dashed) and neutral (black/dotted) years.

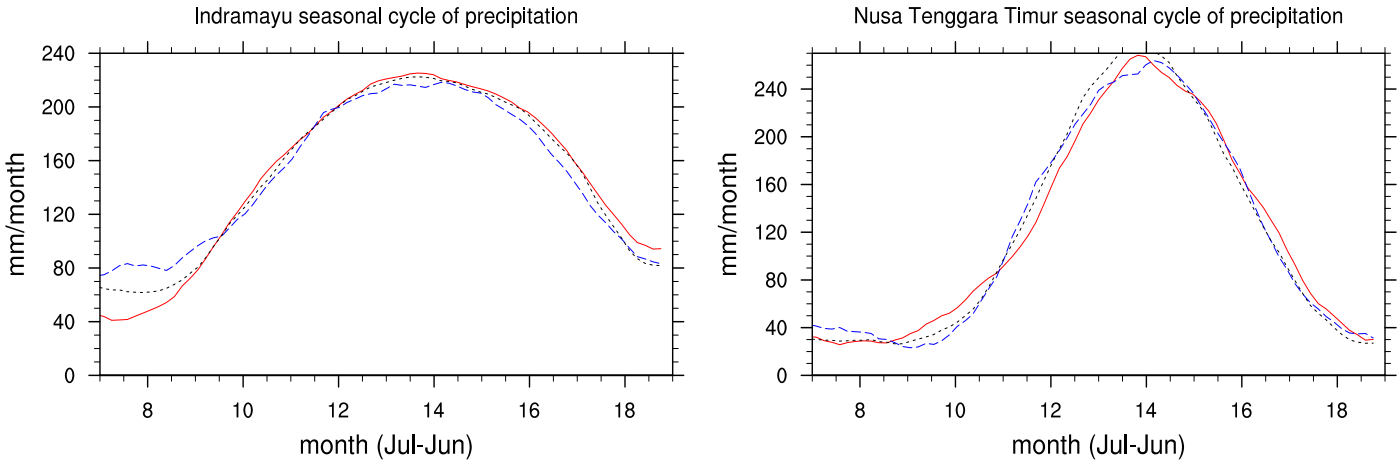

Figure 7: Typical seasonal cycles of precipitation in warm ENSO (red/solid), cold ENSO (blue/dashed) and neutral (black/dotted) years, in Indramayu (left) and Nusa Tenggara Timur (right), as reconstructed using the three leading PCs only.